Zinc and Cadmium Dihydroxide Molecules: Matrix Infrared Spectra and Theoretical Calculations

Xuefeng Wang and Lester Andrews*

Chemistry Department, University of Virginia, P.O. Box 400319, Charlottesville, Virginia 22904-4319

Received: January 20, 2005; In Final Form: February 22, 2005

Laser-ablated zinc and cadmium atoms were mixed uniformly with H_2 and O_2 in excess argon or neon and with O_2 in pure hydrogen or deuterium during deposition at 8 or 4 K. UV irradiation excites metal atoms to insert into O_2 producing OMO molecules (M = Zn, Cd), which react further with H_2 to give the metal hydroxides $M(OH)_2$ and HMOH. The $M(OH)_2$ molecules were identified through O−H and M−O stretching modes with appropriate HD, D_2, $^{16,18}O_2$, and $^{18}O_2$ isotopic shifts. The HMOH molecules were characterized by O−H, M−H, and M−O stretching modes and an M−O−H bending mode, which were particularly strong in pure H_2/D_2. Analogous Zn and Cd atom reactions with H_2O_2 in excess argon produced the same $M(OH)_2$ absorptions. Density functional theory and MP2 calculations reproduce the IR spectra of these molecules. The bonding of Group 12 metal dihydroxides and comparison to Group 2 dihydroxides are discussed. Although the Group 12 dihydroxide O−H stretching frequencies are lower, calculated charges show that the Group 2 dihydroxide molecules are more ionic.

Introduction

Zinc and cadmium dihydroxide are known compounds: $Zn(OH)_2$ is a base with some amphoteric character, and $Cd(OH)_2$ is more basic without the amphoteric property.[1] Solid mercury hydroxide is unknown, but the linear HO−Hg−OH unit exists in an acidified aqua ion Hg^{2+} solution, which is believed to be an extremely weak base.[2] However, chemical comparison with Group 2 dihydroxides shows a different trend: $Be(OH)_2$ is amphoteric, $Mg(OH)_2$ is a base, while the Ca, Sr, and Ba dihydroxides are very strong bases.[1]

The molecular dihydroxides $M(OH)_2$ (M = Zn, Cd) are unknown, but $Hg(OH)_2$ has recently been formed in solid matrixes by this group.[3] In that work, thermally vaporized Hg atoms are co-condensed with O_2 and H_2 in excess argon or neon at low temperature. Subsequently Hg is excited to the ^3P state by mercury arc irradiation, which reacts with O_2 and H_2 in solid argon to give $Hg(OH)_2$.[3] IR spectra and theoretical calculations suggest a linear O−Hg−O structure. Metal hydroxides are formed with little water and water polymer byproduct, and the O−H stretching mode of the major product appeared without contamination. Similar experiments have been done recently with Group 2 metals using laser-ablation technology, and all $M(OH)_2$ (M = Be−Ba) molecules are identified by their OH and O−M−O stretching modes.[4,5] Finally thermal and photolytic reactions of Mg, Ca, Sr, Ba, Zn, Cd, and Hg (M) atoms with H_2O have been investigated, and insertion products HMOH were identified in solid argon.[6,7] However the O−H stretching region is masked by very strong water bands, which prevents observation of this characteristic vibrational mode.

In this paper we report the reactions of Zn and Cd with $O_2 + H_2$ in solid argon and neon. The O−M−O molecules are generated from excited M and O_2, which further react with H_2 giving $M(OH)_2$ and HMOH (M = Zn, Cd). IR spectra are employed to collect molecular vibrational frequency information and theoretical calculations are used to determine molecular spectroscopic and structural properties.

Experimental and Computational Methods

Laser-ablated metal including Zn and Cd atom reactions with oxygen and hydrogen mixtures in excess hydrogen, deuterium, and neon during condensation at 4 K and argon at 8 K have been described in our previous papers.[8−10] The Nd:YAG laser fundamental (1064 nm, 10−20 mJ/pulse, 10 Hz repetition rate with 10-ns pulse width) was focused onto a rotating metal target (Johnson Matthey), which gave a bright ablation plume spreading uniformly to the cold CsI window. The zinc and cadmium targets were filed to remove the oxide coating and immediately placed in the vacuum chamber. FTIR spectra were recorded at 0.5-cm^{-1} resolution on a Nicolet 750 spectrometer with 0.1-cm^{-1} accuracy using a HgCdTe type B detector. Matrix samples were annealed at different temperatures, and selected samples were subjected to photolysis by a medium-pressure mercury arc lamp (Philips, 175W, globe removed).

Experiments were also done using H_2O_2 as the reagent.[11,12] Urea hydrogen peroxide (UHP) (Aldrich, 98%) sample (about 20 mg) was placed between glass wool plugs behind an in-line Teflon−Pyrex needle valve. Argon gas was passed over the UHP sample and co-deposited with metal atoms at 10 K.

Complementary density functional theory (DFT) calculations were performed using the Gaussian 98 program,[13] the B3LYP density functional, and the 6-311++G(3df,3pd) basis set for zinc, hydrogen, and oxygen atoms and Stuttgart/Dresden ECP (SDD) for cadmium. All of the geometrical parameters were fully optimized, and the harmonic vibrational frequencies were obtained analytically at the optimized structures. Additional MP2 calculations were done for comparisons.

Results

IR spectra are presented for zinc and cadmium atom reactions with O_2 and H_2 mixtures in excess argon and neon. Some bands

* To whom correspondence should be addressed. Email: lsa@virginia.edu.

10.1021/jp050362z CCC: $30.25
Published on Web 04/09/2005

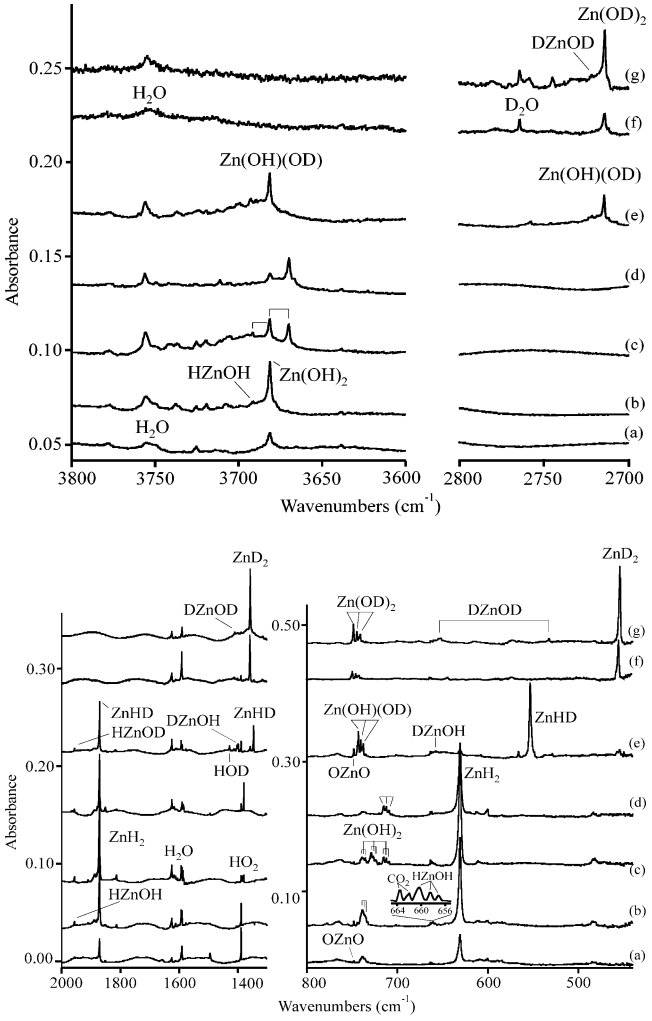

Figure 1. A and B: IR spectra in the 3800−3600-, 2800−2700-, 2000−1300-, and 800−440-cm^{-1} regions for laser-ablated Zn co-deposited with 6% H_2 + 0.4% O_2 in excess argon at 10 K. (a) H_2+O_2 deposition, (b) after λ > 220 nm irradiation, (c) H_2 + $^{16,18}O_2$ deposition followed by λ > 220 nm irradiation, (d) H_2+$^{18}O_2$ deposition followed by λ > 220 nm irradiation, (e) HD + O_2 deposition followed by λ > 220 nm irradiation, and (f) D_2 +O_2 deposition, and (g) after λ > 220 nm irradiation.

are in common and have been observed in previous metal reactions with oxygen or hydrogen in solid matrixes. In the laser ablation process, H−H bonds are broken, and H atoms, H^+, and electrons are produced. The H^+ is trapped in the argon lattice to give Ar_nH^+ and Ar_nD^+ at 903.6 and 643.1 cm^{-1} that have been assigned in early reports.[14,15] The H atom is attached to O_2 to give HO_2 radical (1388.4, 1101.9 cm^{-1}) and D atom to O_2 to give DO_2 (1019.8 cm^{-1}).[16,17] The O_3, O_4^+, O_4^-, and O_6^- ions were also observed as common products as in laser-ablated metal atom reactions with O_2.[18−21] In the solid H_2 and D_2 experiments, H (D) and H^- (D^-) are trapped in solid H_2 (D_2) to form clusters, which have been identified in previous papers.[22,23]

Zn + O_2 + H_2. Figure 1 illustrates IR spectra for laser-ablated Zn reaction with O_2 and H_2 mixture in excess argon after deposition, ultraviolet photolysis, and annealing. A new zinc isotopic triplet contour band appeared at 738.5 cm^{-1} on photolysis and decreased on annealing. The intensity distribution and spacing separation of zinc isotopic triplet bands are almost identical to the absorption of OZnO in solid argon[24] but red shifted about 10 cm^{-1}. A strong band at 3681.5 cm^{-1} in the O−H stretching region tracks the triplet, which can be associated

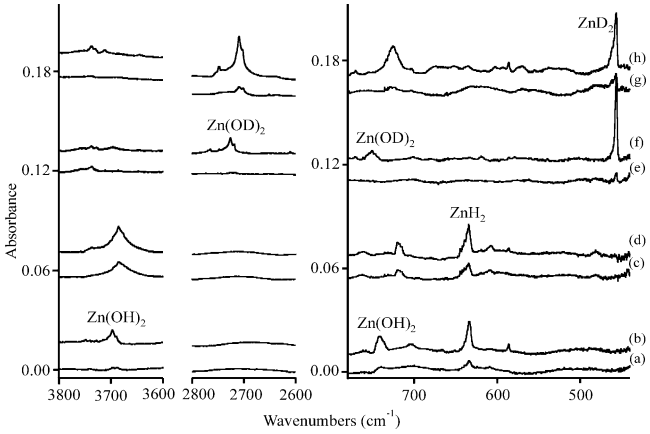

Figure 2. IR spectra in 3800−3600-, 2800−2600-, and 780−440-cm^{-1} regions for laser-ablated Zn co-deposited with 4% H_2 + 0.4% O_2 in excess neon. (a) H_2 + $^{16}O_2$ deposition, (b) after λ > 220 nm irradiation, (c) H_2 + $^{18}O_2$ deposition, (d) λ > 220 nm irradiation, (e) D_2 + $^{16}O_2$ deposition, (f) λ > 220 nm irradiation, (g) D_2 + $^{18}O_2$ deposition, and (h) λ > 220 nm irradiation.

with the same species (group I). Another set of weak bands (group II) at 663.5, 1955.9, and 3691.7 cm^{-1} also appeared on deposition and increased slightly on photolysis. In addition, the reaction of laser-ablated Zn atoms and O_2 + H_2 in excess argon gave absorptions of OZnO at 748.2, 744.4, and 740.9 cm^{-1}, ZnO at 769.2, 766.8, and 764.5 cm^{-1}, ZnH_2 at 1870.2 and 630.5 cm^{-1}, and ZnH at 1493.9 cm^{-1} as observed with each reagent separately.[10,24,25]

For isotopic reagent substitution using $^{16}O_2$ + D_2, the 3681.5-cm^{-1} band shifted to 2714.5 cm^{-1}, but the new triplet band sharpened and showed an unusual blue shift to 748.7, 744.8, and 741.1 cm^{-1} with improved resolution (Figure 1f,g), while group II bands shifted to 2745.1, 1410.3, and 533.2 cm^{-1}, respectively. With $^{16}O_2$ + HD, group I bands at 3681.9 cm^{-1} in the O−H stretching region and 2714.8 cm^{-1} in the O−D stretching region were observed while triplet bands appeared at 743.3, 740.8, and 738.0 cm^{-1}, respectively. A sample of $^{18}O_2$ + H_2 gave ^{18}O shifts for all group I and II bands except the 1955.9-cm^{-1} band. With $^{16,18}O_2$ (20% $^{16}O_2$, 50% $^{16,18}O_2$ and 30% $^{18}O_2$) + H_2, group I bands showed a doublet for upper band and a triplet for lower bands (Figure 1c) and for group II bands a doublet at 3725.5 and 3711.3, 663.5, and 645.3 cm^{-1} associated with 1955.9-cm^{-1} bands were observed. It is not surprising that hydride bands showed no ^{18}O isotopic shifts and oxide bands showed no deuterium shifts.

Similar experiments with selected isotopic substitutions have been done in solid neon, and the spectra are illustrated in Figure 2 and product absorptions are listed in Table 1. With O_2 + H_2 in neon, two new bands at 3696.8 and 745.7 cm^{-1} were produced, and ZnH_2 bands at 1882 and 633 cm^{-1} were generated on λ > 220 nm photolysis. The effect of isotopic substitution on the spectra is also shown in Figure 3. Note that counterpart bands exhibit a several-wavenumber blue shift from argon values and band shapes are broader due to the poor matrix isolation from excess H_2 reagent.

Experiments in solid H_2 and D_2 gave simple results: all metal oxides are reduced, but metal hydroxides and hydrides are trapped. After deposition of Zn with O_2 in H_2, the ZnH_2 (1875.5 and 631.9 cm^{-1}) and ZnH molecules were observed. Also a weak zinc isotopic triplet at 746.3, 744.1, and 741.3 cm^{-1} in the Zn−O stretching region and a band at 3684.6 cm^{-1} in O−H stretching region appeared (Figure 3). UV photolysis (>220 nm) increased these bands by 5-fold, which correspond to group I

TABLE 1: New IR Absorptions (cm^{-1}) Produced on $\lambda > 220$ nm Irradiation of $Zn/O_2/H_2$ Samples in Excess Neon and Argon

$^{16}O_2$, H_2	$^{16,18}O_2$, H_2	$^{18}O_2$, H_2	$^{16}O_2$, HD	$^{16}O_2$, D_2	$^{18}O_2$, D_2	
			Argon			
3691.7	3691.7	3681.1	3691.8, 2722.4	2722.4	2705.4	HZnOH
3681.5	3681.7, 3670.2	3669.9	3681.7, 2714.8	2714.5	2698.0	$Zn(OH)_2$
1955.9	1955.9	1956.1	1955.7, 1410.5	1410.5	1410.3	HZnOH
1870.9	1870.9	1870.9	1870.4, 1346.3	1357.7	1357.7	ZnH_2
1869.7	1869.7	1869.7		1356.5	1356.5	$(ZnH_2)_2$
1868.2	1868.2	1868.2		1355.5	1355.5	$(ZnH_2)_3$
1494.1	1494.1		1494.1, 1087.5	1087.5	1087.5	ZnH
748.2		720.3	748.2		720.3	$O^{64}ZnO$
744.5		716.4	744.5		716.4	$O^{66}ZnO$
738.5	729.2	715.1	743.3	748.7	722.4	$^{64}Zn(OH)_2$
	726.7	712.3	740.8	744.8	718.3	$^{66}Zn(OH)_2$
	724.1	709.0	738.0	741.1	714.4	$^{68}Zn(OH)_2$
				660.2		DZnOD
660.3	660		660.2	533.2	529.1	$H^{64}ZnOH$
658.5						$H^{66}ZnOH$
657.0						$H^{68}ZnOH$
630.6	630.6	630.6	553.0	454.4	454.4	ZnH_2
			Neon			
3696.8		3685.7		2725.9	2709.4	$Zn(OH)_2$
1968.7				1417.8		HZnOH
1882		1882		1365	1365	ZnH_2
830.6		784.6		830.6	784.6	ZnO_3
745.7		720.3		750.6	725.1	$^{64}Zn(OH)_2$
		717.4				$^{66}Zn(OH)_2$
		714.8				$^{68}Zn(OH)_2$
633		633		458	458	ZnH_2

bands observed in solid argon. In addition bands at 665.7, 664.4, and 663.6 cm^{-1} (Zn−O bending), 1963.4 cm^{-1} (Zn−H stretching), 3694.0 cm^{-1} (O−H stretching), and 482.5 and 477.7 cm^{-1} (O−H bending) were generated, which are the counterpart bands of group II in solid argon. With O_2 in solid D_2, the triplet bands of group I shift up to 749.7, 745.9, and 742.2 cm^{-1}, while the triplet bands of group II shift down to 661.5, 659.6, and 657.9 cm^{-1}, which show the same deuterium shift behaviors as in solid argon. Furthermore with O_2/D_2, the O−H and Zn−H stretching modes shift down accordingly and the O−H bending mode moved out of our measurement region. The group I and II bands show slightly different photochemistry: 240−380-nm irradiation favors group I over group II (about 2:1 for the O−D stretching modes), but $\lambda > 220$ nm irradiation allows group II to catch up (Figure 3c). Analogous experiments were done with $^{18}O_2$ in solid H_2 and D_2, and isotopic shifts were observed for all vibrational modes except the Zn−H stretching mode (Table 3).

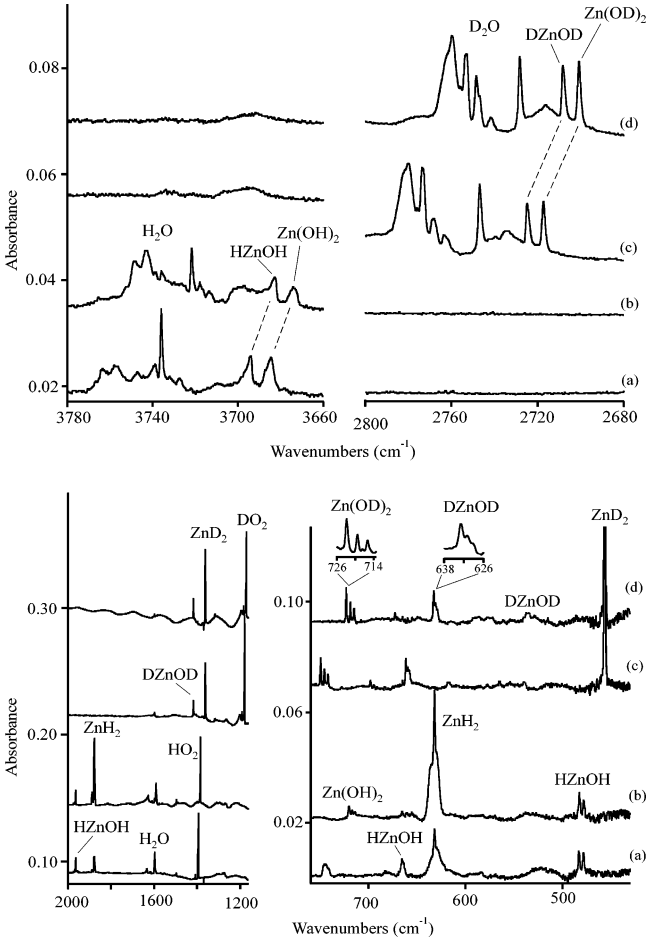

Figure 3. A and B: IR spectra in 3780−3660-, 2800−2680-, 2000−1160-, and 760−430-cm^{-1} regions for laser-ablated Zn co-deposited with 0.2% O_2 in excess hydrogen and deuterium $\lambda > 220$ nm irradiation. (a) O_2 in H_2, (b) $^{18}O_2$ in H_2, (c) O_2 in D_2, and (d) $^{18}O_2$ in D_2.

Cd + O_2 + H_2. IR spectra are shown in Figure 4 for laser-ablated Cd with O_2 and H_2 mixture in excess argon. Absorptions of CdH_2 were observed at 1753.5 cm^{-1} (Cd−H stretching mode) and 601.7 cm^{-1} (H−Cd−H bending mode) and of CdH at 1339.4 cm^{-1} and OCdO at 625.6 cm^{-1}, which have been identified in our early investigations.[10,25] Three new bands appeared at 3658.9, 784.2, and 630.7 cm^{-1} on deposition, increased on ultraviolet photolysis, and decreased on annealing. Experiments with $^{16}O_2 + D_2$ gave large red shifts for the first two bands to 2698.3 and 574.0 cm^{-1} and a small blue shift for last band to 631.9 cm^{-1}. However with $^{18}O_2 + H_2$, the first two bands showed small shifts to 3647.5 and 782.9 cm^{-1}, but the last band shifted to 606.7 cm^{-1}. Additional experiments with $^{16,18}O_2 + H_2$, $^{18}O_2 + D_2$, $O_2 + HD$, and $^{16,18}O_2 + D_2$ were done for band identifications.

Additional weak bands appeared together at 3668.4, 1837.4, 729.1, and 572.0 cm^{-1}, which are very close to the absorptions of HCdOH in solid argon observed by Macrae et al.[7] However, the 3668.4-cm^{-1} band was not reported since the very strong H_2O bands overlapped.

Experiments were performed in solid neon with $O_2 + H_2$, and spectra are shown in Figure 5. Strong absorptions at 1774.3 and 606.5 cm^{-1} are due to CdH_2, and a weak CdH band at 1340.8 cm^{-1} was also observed.[10] New bands at 3672.0, 1842.1, 783.1, 747.8, 638.8, and 556.0 cm^{-1} appeared in the O−H, Cd−

TABLE 2: New IR Absorptions (cm^{-1}) Produced on $\lambda > 220$ nm Irradiation of $Cd/O_2/H_2$ Samples in Excess Neon and Argon

$^{16}O_2$, H_2	$^{16,18}O_2$, H_2	$^{18}O_2$, H_2	$^{16}O_2$, HD	$^{16}O_2$, D_2	$^{16,18}O_2$, D_2	$^{18}O_2$, D_2	
			Argon				
3668.4		3658.5	3668.4, 2705.1	2705.3		2688.8	HCdOH
3658.9	3658.9, 3647.5	3647.5	3659.3, 2698.5	2698.3	2698.3, 2682.1	2682.1	$Cd(OH)_2$
1837.5	1837.4	1837.4	1837.4, 1320.4	1320.4	1320.4	1320.4	HCdOH
1753.5	1753.5	1753.5	1756.9, 1260.7	1264.4	1264.4	1264.4	CdH_2
1339.4	1339.4	1339.4	1339.4, 974.4	974.4	974.4	974.4	CdH
784.2	782.9	781.4	786.4, 579.4	573.5	573.5	550.3	$Cd(OH)_2$
729.1	728.8	728.4	727.4, 572.2				HCdOH
630.8	619.0	masked	631.0	631.9	621.2	604.9	$^{112}Cd(OH)_2$
629.6	617.8				620.2	603.8	$^{114}Cd(OH)_2$
625.6	613.3	598.0	625.6	625.6	613.3	598.0	OCdO
604.6	604.6	604.6	530.0	434.2	434.2	434.2	CdH_2
601.7	601.7	601.7	527.5	432.5	432.5	432.5	CdH_2 site
572.0	572, 544	544.5		547.6		522.8	HCdOH
			Neon				
3672.0		3660.4		2708.4		2691.8	$Cd(OH)_2$
1774.3		1774.3		1280.4		1280.4	CdH_2
1340.8		1340.8					CdH
1842.1		1842.1		1324.3			HCdOH
822.6		775.4		822.6		778.1	CdO_3
783.1		782.6					$Cd(OH)_2$
747.8				602.2			HCdOH
638		611		638		611	$Cd(OH)_2$
606.5		606.5		437.4		437.4	CdH_2
556.0		530.1		553.7		527.4	X(OCdO)

TABLE 3: New IR Absorptions (cm^{-1}) Produced on $\lambda > 220$ nm Irradiation of $Zn/O_2/H_2$ and $Cd/O_2/H_2$ Samples

Zn					Cd				
O_2/H_2	$^{18}O_2/H_2$	O_2/D_2	$^{18}O_2/D_2$	assignment	O_2/H_2	$^{18}O_2/H_2$	O_2/D_2	$^{18}O_2/D_2$	assignment
3694.0	3682.9	2724.8	2708.2	HZnOH	3671.8	3659.7	2708.1	2691.5	HCdOH
3684.6	3673.8	2717.3	2700.8	$Zn(OH)_2$	3660.6	3649.8	2700.5	2684.1	$Cd(OH)_2$
1963.4	1963.4	1416.1	1416.1	HZnOH	1841.5	1841.5	1324.6	1324.6	HCdOH
1875.5	1875.5	1361.5	1361.5	ZnH_2	1762.5	1762.5	1270.1	1270.1	CdH_2
1495.4	1495.4	1091.1	1091.1	ZnH	1340.4	1340.4	978.7	978.7	CdH
746.6	720.5	749.7	723.2	$^{64}Zn(OH)_2$	632.8		633.3	606.6	$Cd(OH)_2$
744.1	717.1	745.9	719.2	$^{66}Zn(OH)_2$	793.0				$Cd(OH)_2$
741.5	714.1	742.2	715.3	$^{68}Zn(OH)_2$	733.6		578.0	556.3	HCdOH
665.7	masked	661.5	632.8	$H^{64}ZnOH$	573.0	546.6			HCdOH
664.2	masked	659.6	630.9	$H^{66}ZnOH$					
663.6	masked	657.9	629.0	$H^{68}ZnOH$					
		539.2	535.2	DZnOD					
632.1	632.1	456.0	456.0	ZnH_2	604.5	604.5	435.4	435.4	CdH_2
482.5	482.2			HZnOH	457.3				HCdOH
477.7	477.6			HZnOH	453.9				HCdOH

H, and Cd−O stretching regions. On annealing a very strong cadmium ozonide band appeared at 822.6 cm^{-1}.

Analogous experiments were done in pure H_2 and D_2, and product absorptions are listed in Table 3. The oxide bands (CdO, CdO_2, CdO_3) were not observed, suggesting all oxides were reduced by hydrogen to form hydroxides, as shown in Figure 6.

Figure 7 compares IR spectra for Zn, Cd, and Hg reactions with O_2 and H_2 in excess argon and neon. Note the Group 12 family trends.

M + H_2O_2. Complementary experiments were done with laser-ablated Zn and Cd reacting with H_2O_2 in a flowing argon stream, and IR spectra are compared in Figure 8. Strong H_2O_2 bands were observed at 3597, 3587, and 1270.8 cm^{-1}.[11] The Zn product bands at 3681.4 and 739.3 cm^{-1} were sharper, and zinc isotopic splittings were resolved on the latter at 737.1 and 735.0 cm^{-1}. Irradiation at 240−380 nm increased each band by 25%, and further irradiation at $\lambda > 220$ nm increased each band another 20%. Additional weak bands were observed at 1956.4 and 660.2 cm^{-1}. The hard radiation from the Zn ablation plume photodissociated some H_2O_2 into the HOH···O complex with absorptions at 3730, 3725.3 (site), 3633, and 3630.1 (site) cm^{-1},[12] and HO_2 radical was also observed. The analogous investigation with Cd gave bands at 3658.9, 783.4, 630.9, and 629.6 cm^{-1}, which increased together on UV irradiation and displayed the ^{112}Cd and ^{114}Cd isotopic contours for the latter band. Annealing to 33 K sharpened these bands and enhanced the cadmium isotopic splittings now at 631.4, 630.3, 629.1, and 627.9 cm^{-1} for the ^{110}Cd, ^{112}Cd, ^{114}Cd, and ^{116}Cd products. In addition, weak bands were observed at 3669.9, 1837.3, and 729 cm^{-1}. Another experiment was done with a fresh UHP charge, the H_2O_2 absorptions were 2.5 times as strong, and the product absorptions were 50% more intense: Spectra from the latter experiment are illustrated in Figure 8.

To complement and strengthen our earlier identification of $Hg(OH)_2$,[3] new experiments were done with Hg and H_2O_2. Figure 8a shows the spectrum of Hg vapor co-deposited with argon/H_2O_2, and no products were formed. Irradiation at 240−380 nm had no effect, but irradiation with the full light of the mercury arc produced new absorptions at 3629.0, 927.0, and 637.1 cm^{-1} with twice the intensity and in excellent agreement with the 3629.4-, 927.1-, and 637.3-cm^{-1} absorptions assigned to $Hg(OH)_2$ from the Hg, O_2, and H_2 photochemical reaction.[3] Note that the photodissociation of H_2O_2 and the yield of the

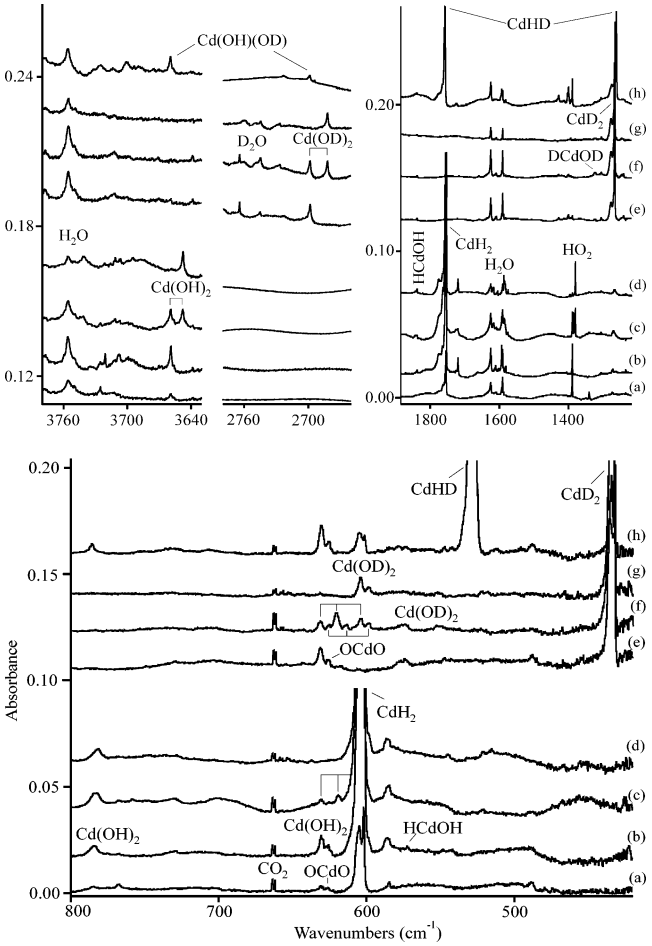

Figure 4. A and B: IR spectra in 3780−3630-, 2780−2660-, 1900−1220-, and 800−420-cm^{-1} regions for laser-ablated Cd co-deposited with 6% H_2 + 0.4% O_2 in excess argon. (a) H_2+O_2 deposition, (b) after λ > 220 nm irradiation, (c) H_2 + $^{16,18}O_2$ deposition and λ > 220 nm irradiation, and likewise for (d) H_2 + $^{18}O_2$, (e) D_2 + O_2, (f) D_2 + $^{16,18}O_2$, (g) D_2 + $^{18}O_2$, and (h) HD +O_2.

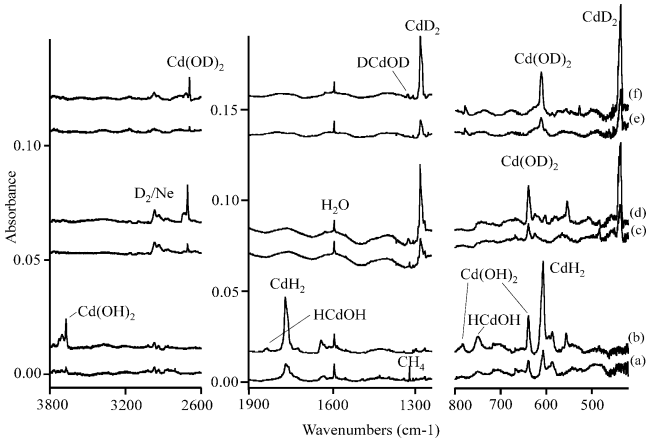

Figure 5. IR spectra in 3900−2600-, 1900−1240-, and 780−440-cm^{-1} regions for laser-ablated Cd co-deposited with 4% H_2 + 0.4% O_2 in excess neon. (a) H_2 + O_2 deposition, (b) after λ > 220 nm irradiation, (c) D_2 + O_2 deposition, (d) after λ > 220 nm irradiation, (e) D_2 + $^{18}O_2$ deposition, and (f) after λ > 220 nm irradiation.

HOH···O complex are greatly reduced, the 3725.3-cm^{-1} HOH···O site splitting is weaker than in Figure 8i, and the contribution at 3630.1 cm^{-1} is expected to be even weaker. Hence, most of the sharp absorption at 3629.0 cm^{-1} is due to $Hg(OH)_2$.

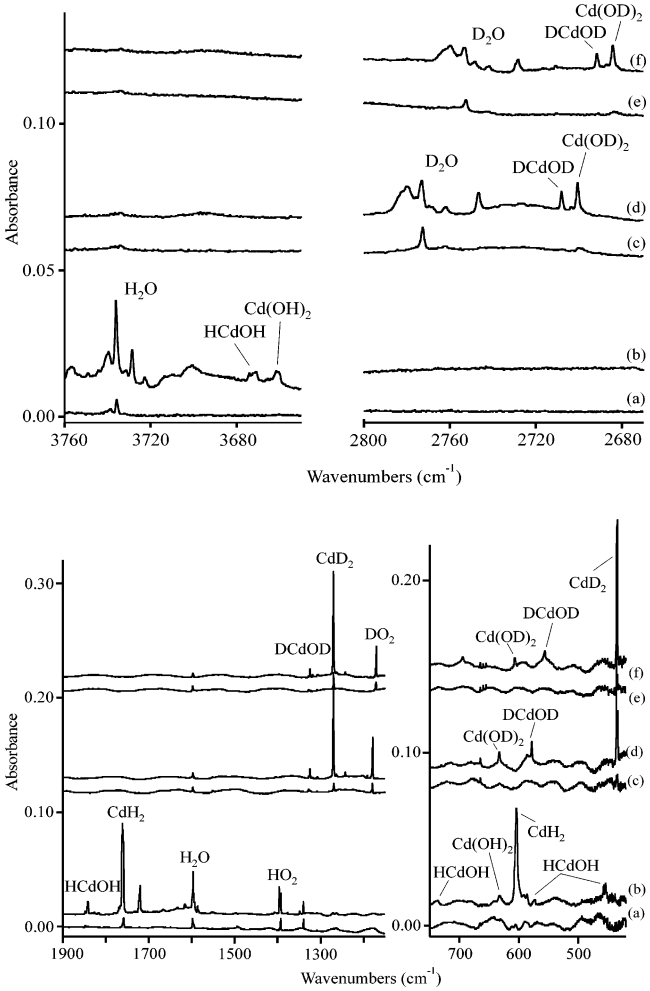

Figure 6. A and B: IR spectra in 3760−3650-, 2800−2670-, 1900−1150-, and 750−420-cm^{-1} regions for laser-ablated Cd co-deposited with 0.2% O_2 in excess hydrogen and deuterium. (a) O_2 in H_2 deposition, (b) after λ > 220 nm irradiation, (c) O_2 in D_2 deposition, (d) after λ > 220 nm irradiation, (e) $^{18}O_2$ in D_2 deposition, and (f) after λ > 220 nm irradiation.

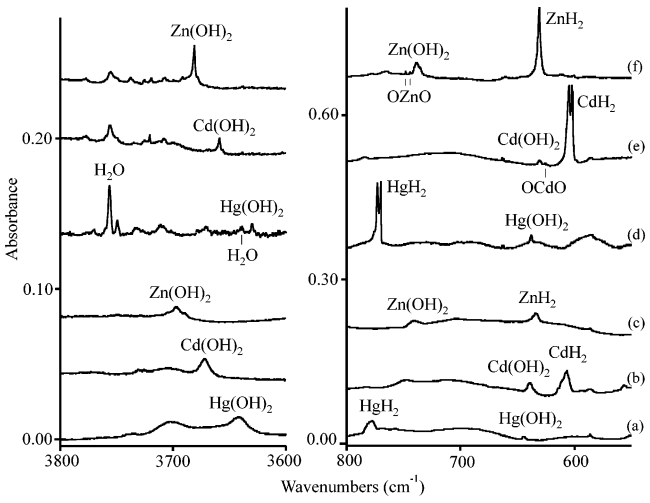

Figure 7. IR spectra in the 3000−3600- and 800−550-cm^{-1} regions comparing the products of ultraviolet photochemical reactions of Zn, Cd, and Hg with O_2 + H_2 in excess argon and neon. (a) Hg in Ne, (b) Cd in Ne, (c) Zn in Ne, (d) Hg in Ar, (e) Cd in Ar, and (f) Zn in Ar.

Calculations. Calculations were done for $Zn(OH)_2$ and $Cd(OH)_2$ at the B3LYP and MP2 levels of theory, and the structures are illustrated in Figure 9. These molecules have the C_2

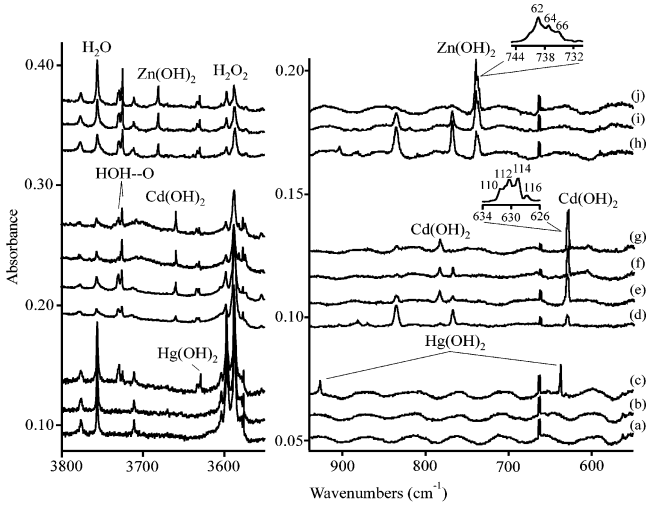

Figure 8. IR spectra in the 3800−3550- and 950−550-cm^{-1} regions comparing the products of ultraviolet photochemical reactions of Zn, Cd, and Hg with H_2O_2 in excess argon. (a) Hg vapor deposited from 50 °C liquid for 60 min, (b) after 240−380 nm irradiation, (c) after λ > 220 nm irradiation, (d) laser-ablated Cd deposited for 40 min, (e) after λ > 220 nm irradiation, (f) after annealing to 22 K, (g) after a second λ > 220 nm irradiation, (h) laser-ablated Zn deposited for 40 min, (i) after 240−380 nm irradiation, and (j) after λ > 220 nm irradiation. The 835.3- and 767.6-cm^{-1} absorptions are common to H_2O_2 subjected to radiation from laser ablation of metal targets.

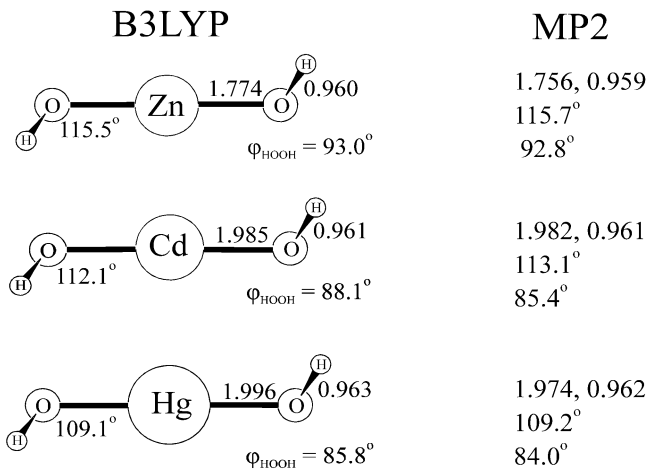

Figure 9. Structures of Group 12 dihydroxide molecules computed at the B3LYP and MP2 levels using the 6-311++G(3df, 3pd) basis for H, O, and Zn and the SDD pseudopotential for Cd and Hg. Bond distances in angstrom units.

symmetry of the parent H_2O_2 molecule, which is shared with $Be(OH)_2$ and $Hg(OH)_2$ but not with the dihydroxides of Ca, Sr, and Ba.[3−5] Calculated frequencies are listed in Table 4. Also included are other important molecules that relate to this system.

Discussion

Assignment of Zn and Cd hydroxides will be presented based on isotopic shifts in the IR spectrum and theoretical calculations of vibrational frequencies.

$Zn(OH)_2$. In solid argon new triplet absorptions at 739.3, 737.1, and 735.0 cm^{-1} (from more dilute reagent H_2O_2 experiment) track the 3681.5-cm^{-1} band on photolysis and annealing. The new triplet pattern is appropriate for ^{64}Zn, ^{66}Zn, and ^{68}Zn in natural abundance where only one Zn atom is involved in this molecule: A similar zinc isotopic pattern was observed for OZnO.[24] The triplet shifts to 715.1, 712.3, and 709.0 cm^{-1}, and the 3681.5-cm^{-1} band shifts to 3669.9 cm^{-1} in the $^{18}O_2 + H_2$ experiment. This shows that the lower bands are Zn−O stretching while the upper one is due to O−H stretching motions. The oxygen isotopic triplet pattern for the lower mode with $^{16}O_2 + {}^{16}O^{18}O + {}^{18}O_2 + H_2$ shows that two equivalent oxygen atoms are involved, and a doublet was observed for the O−H stretching mode with the same sample. Very similar isotopic patterns were observed for Group 2 metal dihydroxides $M(OH)_2$ (M = Be, Mg, Ca, Sr, and Ba)[4,5] and $Hg(OH)_2$,[3] and $Zn(OH)_2$ is assigned accordingly. This identification is substantiated by observation of the same bands with the $O_2 + H_2$ and H_2O_2 reagents.

With $O_2 + D_2$, the Zn−O stretching mode blue shifts about 10 cm^{-1} to 748.7, 744.8, and 741.1 cm^{-1}, indicating strong coupling of the O−D bending vibration with this mode. The O−D stretching mode appeared at 2714.5 cm^{-1}, giving a 1.3565 H/D ratio, which is very close to the ratio found for Group 2 metal dihydroxides[4,5] and $Hg(OH)_2$.[3] In addition, the 16/18 ratio, 1.00316, is near that found for $Ca(OH)_2$, namely, 1.00323, which also has a similar H/D ratio (1.3555). With $O_2 + HD$, two bands were observed at 3681.7 and 2714.8 cm^{-1} for a molecule with OH and OD groups. The lack of a shift from $Zn(OH)_2$ means that very little coupling occurs between two equivalent O−H groups. Finally, the Zn−O stretching mode, 743.3 cm^{-1}, was found near the average of H_2 and D_2 reagent values.

In solid hydrogen, the absorptions of $Zn(OH)_2$ were observed at 3684.6 cm^{-1} (O−H stretching) and 746.3, 744.1, and 741.3 cm^{-1} (Zn−O stretching), slightly higher than the argon matrix values. With O_2 in solid D_2, the O−H stretching mode shifts to 2717.3 cm^{-1}, giving the H/D = 1.3560 ratio, which is in line with the argon value. The blue shifts of the Zn−O stretching mode of $Zn(OD)_2$ also correspond with argon values. With $^{18}O_2$ in solid H_2 the Zn−O modes shift to 720.4, 717.0, and 714.1 cm^{-1}, giving a 1.0360 $^{16}O/^{18}O$ ratio, which is slightly higher than in argon and can be reasoned by interaction of Zn−O−H with H_2. The $Zn-O^{\delta-}-H^{\delta+}\cdots H-H$ interaction results in slightly more Zn−O vibrational motion than in free Zn−O−H.

The neon matrix counterparts of both $Zn(OH)_2$ and $Zn(OD)_2$ absorptions are blue shifted slightly, to 3696.8 and 2725.9 cm^{-1}, which is the normal relationship for matrix shifts dominated by polarizability-based dispersive interactions. The assignment is further supported by neon matrix observations of 745.7 cm^{-1} (Zn−O stretching) with $H_2 + O_2$ and 725.1 cm^{-1} with $D_2 + O_2$. The O−H mode gives a 1.3562 H/D ratio that is almost identical to the argon value. However the zinc isotopic information is lost for the O−Zn−O stretching mode because of band broadness. Additional experiments with $H_2 + {}^{18}O_2$ gave 3685.7 and 720.3 cm^{-1} and with $D_2 + {}^{18}O_2$ produced 2709.4 and 725.1 cm^{-1}, which are in excellent correspondence with argon spectra. Complementary information is obtained in solid H_2 and D_2, where the O−H and O−D stretching modes (Figure 3A) are between neon and argon matrix values and the Zn−O stretching modes exhibit resolved isotopic splittings for a single Zn atom (Figure 3B).

The identification of $Zn(OH)_2$ is supported by B3LYP and MP2 calculations. The calculations suggest a structure with a linear O−Zn−O subunit and two H located off axis at 115.5° with a dihedral angle of 93° and C_2 symmetry. The predicted Zn−O stretching frequency at 750.3 cm^{-1} (B3LYP) and 747.3 cm^{-1} (MP2) is in excellent agreement with the observed value of 738.5 cm^{-1}. The antisymmetric O−H stretching mode (B symmetry) is calculated at 3872.1 cm^{-1} (B3LYP) and 3925.1 cm^{-1} (MP2), which are overestimated by 5.2 and 6.6%, respectively, which is consistent within prediction error of O−H stretching modes in metal hydroxides.[5] The blue shift in the

TABLE 4: Calculated Frequencies for M(OH)$_2$, OMO, HMOH, and MOH (M = Zn and Cd) at B3LYP Level of Theory

Zn(OH)$_2$[a]		Zn(^{18}OH)$_2$		Zn(OD)$_2$		OZnO[b]		HZnOH[c]		ZnOH[d]	mode[e]
calcd	obsd	calcd	obsd	calcd	obsd	calcd	obsd	calcd	obsd	calcd	
3872.9 (A, 13)		3860.1 (12)		2819.9 (9)				3887.6 (48)	3691.7		O−H s-str
3872.1 (B, 94)	3681.5	3859.4 (91)	3669.9	2819.2 (63)	2714.5			1990.7 (83)	1955.9	3832.5 (39)	O−H a-str
790.0 (B, 22)		785.5 (38)		619.6 (6)				722.7 (46)			Zn−O−H bend
785.3 (A, 21)		782.1 (20)		577.0 (59)							Zn−O−H bend
750.3 (B, 213)	738.5	723.6 (185)	715.1	755.1 (131)	748.7	797.7 (47)	748.2	664.2 (102)	660.3	712.2 (36)	Zn−O a-str
607.3 (A, 0)						633.8 (0)		479.8 (57)	482.5		Zn−O s-str
175.9 (A, 9)											
159.9 (B, 9)											
137.6 (A, 102)						166.7 (312)		460.3 (66)	477.7	552.0 (59)	O−Zn−O bend

Cd(OH)$_2$[a]		Cd(^{18}OH)$_2$		Cd(OD)$_2$		OCdO[b]		HCdOH[c]		CdOH[d]	mode[e]
calcd	obsd	calcd	obsd	calcd	obsd	B3LYP	obsd	calcd	obsd	calcd	
3849.2 (A, 9)		3836.5 (8)		2802.5 (6)				3863.0 (37)	3668.4		O−H s-str
3848.5 (B, 86)	3658.9	3835.8 (83)	3647.5	2801.7 (57)	2698.3			1911.8 (118)	1837.4	3807.3 (40)	O−H a-str
830.9 (A, 9)		827.6 (18)		616.3 (13)				766.4 (57)	729.1		Cd−O−H bend
823.1 (B, 78)	784.2	820.0 (72)	781.4	586.2 (10)				562.8 (65)	572.0		Cd−O−H bend
617.4 (B, 114)	630.7	590.7 (107)		630.3 (152)	631.9	632.9 (36)		479.3 (46)	457.3	733.7 (43)	Cd−O a-str
524.6 (A, 0)						536.7 (0)	625.6				Cd−O s-str
145.8 (A, 3)											
127.1 (B, 5)											
104.1 (A, 89)						132.5 (262)		448.4 (59)	453.9	444.3 (27)	O−Cd−O bend

[a] Structural parameters given in Figure 9. Frequencies, cm^{-1} (intensities, km/mol). Irreducible representations in C_2 point group given for Zn(OH)$_2$ and Cd(OH)$_2$. [b] Linear molecules: Zn−O, 1.733 Å; Cd−O, 1.931 Å. [c] Planar molecules: H−Zn, 1.512 Å; Zn−O, 1.783 Å; O−H, 0.959 Å; H−Zn−O, 175.8°; Zn−O−H, 118.4°; H−Cd, 1.644 Å; Cd−O, 1.996 Å; O−H, 0.960 Å; H−Cd−O, 176.1°; Cd−O−H, 114.4°. [d] Zn−O, 1.839 Å; O−H, 0.963 Å; Zn−O−H, 113.6°; Cd−O, 2.089 Å; O−H, 0.965 Å; Cd−O−H, 109.5°. [e] Mode description for M(OH)$_2$ molecules.

antisymmetric stretching mode from interaction with the H(D)−O−Zn−O−(D)H bending mode is also predicted. Note that the O−Zn−O stretching mode for free OZnO is calculated at 797.7 cm^{-1} (B3LYP), which is 49.5 cm^{-1} higher than the argon matrix value, partly because of a stronger interaction of the triplet OZnO molecule with the argon matrix.

Cd(OH)$_2$. Three bands at 3658.9, 784.2, and 630.8 cm^{-1} track together on irradiation and annealing in Cd + O_2 + H_2 reactions in solid argon. With O_2 + D_2, these bands appeared at 2698.3, 631.9, and 573.5 cm^{-1}, respectively. The H/D ratios (3658.9/2698.3 = 1.3560 and 784.2/573.5 = 1.3674) show that the 3658.9 cm^{-1} band is primarily a hydrogen motion, which is appropriate for the O−H stretching mode. The 630.7-cm^{-1} band shifts up 1.2 cm^{-1} in the same experiment, and this mode must be assigned to a metal−oxygen vibration. With $^{18}O_2$ + H_2, two upper bands have very slight shifts (3647.7 and 781.4 cm^{-1}, respectively), but the 630.7-cm^{-1} band moved under the CdH_2 band at 604.6 cm^{-1}, which clearly suggests a metal−oxygen stretching mode assignment. Experiments with $^{16}O_2$/$^{16}O^{18}O$/$^{18}O_2$ + H_2 gave the first two bands of a triplet distribution denoting the vibration of two equivalent oxygen atoms. Experiments with $^{18}O_2$ + D_2 and $^{16,18}O_2$ + D_2 provided additional isotopic data for this molecule: Doublet bands at 2682.1 and 2698.3 cm^{-1} and triplet bands at 631.9, 620.4, and 604.5 cm^{-1} confirm the cadmium dihydroxide assignment. Accordingly, the 3658.9-, 784.2-, and 630.8-cm^{-1} bands are assigned to the Cd(OH)$_2$ molecule, which is substantiated by observation of essentially the same absorptions for the Cd + H_2O_2 reaction. The 630.8-cm^{-1} absorption is sharp enough in the latter spectrum (Figure 8) to give a partially resolved natural cadmium isotopic distribution[10,24] that is characteristic of a single Cd atom vibration.

Assignment of 3658.9, 784.2, and 630.8 cm^{-1} bands to the Cd(OH)$_2$ molecule is supported by B3LYP and MP2 theoretical calculations. The geometry of Cd(OH)$_2$ is very similar to Zn(OH)$_2$ with slightly longer Cd−O and O−H bond length and smaller dihedral angle. The strong antisymmetric (B symmetry) O−H stretching and O−Cd−O stretching modes for Cd(OH)$_2$ are predicted at 3848.5 and 617.4 cm^{-1} at the B3LYP level with +5.2 and −2.1% error, which reproduce the observed values very well. In addition, the Cd−O−H bending mode is calculated at 823.1 cm^{-1} with +5.0% error. The calculated O−D stretching, O−Cd−O stretching, and Cd−O−D bending modes of Cd(OD)$_2$ are at 2801.7, 630.3, and 586.2 cm^{-1}, respectively, but the 586.2 cm^{-1} band loses IR intensity by 8-fold, which is in very good agreement with experimental observations.

In solid neon, absorptions of Cd(OH)$_2$ appear at 3672.0, 783.1, and 638 cm^{-1} and Cd(OD)$_2$ at 2708.4 and 638 cm^{-1}. Note that the O−Cd−O stretching mode was essentially not shifted, while the bending Cd−O−D mode was not observed. With $^{18}O_2$ substitution, all bands shift accordingly. The pure H_2-doped O_2 sample gave IR absorptions at 3660.6, 793.0, and 632.8 cm^{-1}, which are assigned to Cd(OH)$_2$, and pure D_2 gave counterpart bands for Cd(OD)$_2$ at 2700.5 and 633.3 cm^{-1}. Additional experiments with $^{18}O_2$ + H_2 and $^{18}O_2$ + D_2 gave appropriate ^{18}O isotopic shifts.

HZnOH. Two weak bands at 1955.3 (site at 1965.3) and 660.3 cm^{-1} tracked in the Zn atom reaction with O_2 and H_2 mixture in solid argon, which were assigned to HZnOH by Greene et al. and Macrae et al. in the reaction of Zn with H_2O in solid argon.[7,25] An additional weak 3691.7-cm^{-1} band in the O−H stretching region shows the same annealing and photolysis behavior and can be assigned to the OH stretching mode for HZnOH, and the deuterium counterpart was found at 2722.4 cm^{-1} giving the 1.356 H/D ratio. With $^{18}O_2$ + H_2, the upper band shifted to 3681.8 cm^{-1} and the lower band shifted under ZnH_2 (Zn−O stretching region). With $^{16}O_2$ + HD, the spectra show two bands at 3691.8 and 2722.4 cm^{-1} (O−H and O−D stretching) and two bands at 1955.7 and 1410.7 cm^{-1} (Zn−H and Zn−D stretching). All of this spectral information supports the HZnOH assignment.

The solid H_2 and D_2 experiments gave clear O−H (O−D), Zn−H (Zn−D), and Zn−O stretching vibrations for HZnOH (DZnOD). A zinc isotopic triplet at 665.7, 664.2, and 663.6 cm^{-1} in O_2/H_2 shifts to 661.5, 659.6, and 657.9 cm^{-1} in O_2/D_2 and shifts to 632.8, 630.9, and 629.0 cm^{-1} in $^{18}O_2$/D_2, which is

assigned to the Zn−O stretching modes in HZnOH (DZnOD). However this mode is overlapped with the ZnH_2 bending mode in $^{18}O_2/H_2$ experiments. In addition, the Zn−H and O−H stretching modes were observed at 1963.4 and 3694.0 cm^{-1}, respectively, which shifts to 1416.1 and 2724.8 cm^{-1} with O_2 in solid D_2. In p-H_2, the strong Zn−H stretching mode was resolved into a zinc isotopic triplet,[10] which further shows that a single Zn atom is involved. Furthermore the O−H bending modes at 482.5 and 477.7 cm^{-1} with O_2 in solid H_2 were observed but the deuterium counterparts shift out of our measurement region. The 2724.8 and 2717.3 cm^{-1} bands for DZnOD and $Zn(OD)_2$ clearly show different ultraviolet photochemical behavior. In solid neon the product bands are broader, and new bands at 1968.3 and 666.5 cm^{-1} in the Zn reaction with $H_2 + O_2$ are appropriate for HZnOH.

DFT frequency calculations predict O−H stretching at 3887.6 cm^{-1}, Zn−H stretching at 1990.7 cm^{-1}, and Zn−O stretching at 664.2 cm^{-1}, which match the experimental observations nicely. The calculated O−H stretching vibration in HZnOH is 15.5 cm^{-1} higher than in $Zn(OH)_2$ and the Zn−O vibration in HZnOH is 86.1 cm^{-1} lower than in $Zn(OH)_2$, which are in good agreement with our observations.

HCdOH. The absorptions due to HCdOH in argon at 1837.4 (Cd−H stretching), 729.1 (Cd−O−H bending), and 572.0 cm^{-1} (Cd−O stretching) are basically the same as the frequencies reported by Greene et al.[25] and Macrae et al.[7] However the O−H stretching frequency was not observed for this molecule in Cd + H_2O reactions. With $O_2 + H_2$ in solid argon, a weak band at 3668.4 cm^{-1} tracks the lower bands and is appropriate for the O−H stretching mode, as it shifts to 3647.5 cm^{-1} with ^{18}O substitution and to 2698.3 cm^{-1} with deuterium (H/D = 1.360).

In solid neon, bands at 1842.1 and 747.8 cm^{-1} appeared on deposition and increased on photolysis. These bands correspond to argon values of HCdOH very well, and the assignment is straightforward.

The experimental assignments to HCdOH and DCdOD are confirmed by the solid H_2 and D_2 experiments (Figure 6). The higher-frequency 3671.8 and 2708.1 cm^{-1} bands for O−H and O−D stretching modes track with lower-frequency 1841.5 and 1324.6 cm^{-1} bands for Cd−H and Cd−D vibrations: 733.6 and 578.0 cm^{-1} for Cd−O−H and Cd−O−H bending and a 573.0 cm^{-1} band for the O−Cd−O stretching mode for HCdOH.

These assignments are supported by DFT frequency calculations. First, the O−H stretching mode of HCdOH is predicted to be 14.5 cm^{-1} higher than that for $Cd(OH)_2$, and we observe it 11.2 cm^{-1} higher (solid hydrogen). Second, the Cd−O stretching mode for HCdOH is computed to be 54.6 cm^{-1} lower than that for $Cd(OH)_2$, and we observe it 58.7 cm^{-1} lower. Third, the Cd−O−H bending mode predicted at 766.4 cm^{-1} with increased intensity and is observed for HCdOH at 729.1 cm^{-1}.

Bonding in Metal Dihydroxides. The O−H stretching frequencies of molecular metal hydroxides are often related to ionic character[26−28] since more charge transfers to OH from the metal reducing the O−H bond strength. For example the Group 2 metal dihydroxide O−H stretching frequencies at 3829.8 cm^{-1} for $Mg(OH)_2$, 3784.6 cm^{-1} for $Ca(OH)_2$, 3760.6 cm^{-1} for $Sr(OH)_2$, and 3724.2 cm^{-1} for $Ba(OH)_2$, in solid argon continuously decrease as ionic character increases. This is consistent with Mulliken charges +1.29 (Mg), +1.72 (Ca), +1.75, (Sr), and +1.74 (Ba), although Mulliken charge is an overestimate of the actual charge.[5] However, the O−H stretching frequencies of $Zn(OH)_2$, $Cd(OH)_2$, and $Hg(OH)_2$ at 3681.5, 3658.9, and 3629.4 cm^{-1} and Mulliken charges +0.78 (Zn), +1.52 (Cd), and +1.41 (Hg) both decrease in the $Zn(OH)_2$, $Cd(OH)_2$, and $Hg(OH)_2$ group. Therefore ionic character is not the only consideration.

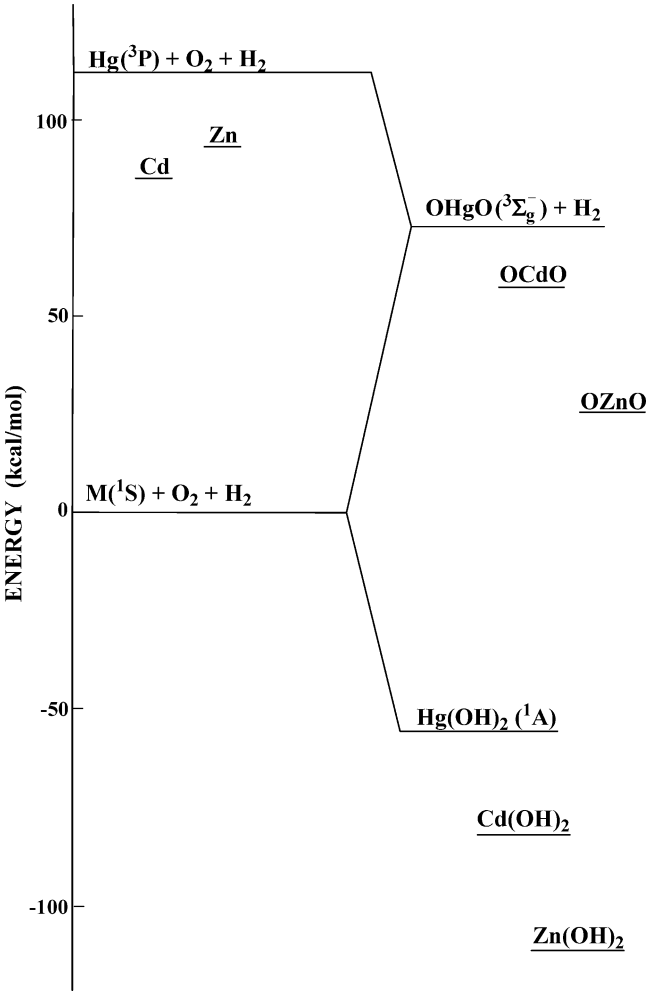

Figure 10. Relative energies computed at the B3LYP level using the 6-311++G(3df, 3pd) basis for H, O, and Zn and SDD for Cd and Hg for important Zn, Cd, and Hg oxide and dihydroxide species.

The ionic limit can be considered at 3644 cm^{-1}, as represented by solid $Ca(OH)_2$, or better yet 3555.6 cm^{-1}, as represented by gaseous OH^-.[29,30] However, the neutral OH radical fundamental frequency, 3568 cm^{-1}, falls in this region as well.[31] So the position of the O−H stretching frequency is not in itself a measure of charge on the OH moiety. The structures of $Zn(OH)_2$, $Cd(OH)_2$, and $Hg(OH)_2$, particularly the linear O−M−O linkage and the 115−109° M−O−H angles (Figure 9), argue for considerable covalent character. In marked contrast, the $Sr(OH)_2$ and $Ba(OH)_2$ molecules are bent at the metal centers, the M−O−H subunits are linear, and the molecules have considerable ionic character.[5,32]

Natural orbital analysis was done on the Group 2 and 12 $M(OH)_2$ molecules for comparison. The Ca, Sr, and Ba species have *n*s populations of 0.01 e and *n*d populations of 0.09−0.12 e, but in contrast Zn in $Zn(OH)_2$ has $4s^{0.52}$ $3d^{9.91}$ valence population, Cd in $Cd(OH)_2$ has $5s^{0.59}$ $4d^{9.90}$, and Hg in $Hg(OH)_2$ has $6s^{0.92}$ $5d^{9.79}$. Clearly slightly higher 6s population in $Hg(OH)_2$ suggests more back electron donation from OH^-, indicating significant covalent character, and in aqueous solution HgO precipitates to form solid zigzag −O−Hg−O−Hg− chains.[1,2] The effect of 10 *n*d electrons on the bonding and structure of Group 12 relative to Group 2 $M(OH)_2$ molecules is straightforward.

The O−H fundamentals for $Zn(OH)_2$ at 3681.5, 3684.6, and 3696.8 cm^{-1} in solid argon, hydrogen, and neon, respectively, show the normal relationship for matrix shifts. Similar observations for $Cd(OH)_2$ at 3658.9, 3660.6, and 3672.0 cm^{-1} and for $Hg(OD)_2$ at 2677.7, 2679.6, and 2684.0 cm^{-1}[13] in solid argon, deuterium, and neon, respectively, follow the same pattern.

Reaction Mechanisms. The stable Group 12 $M(OH)_2$ molecules are formed in considerable yield from the photoexcited metal atom reaction with O_2 and H_2 mixtures. The ultraviolet excitation is sufficient to access the ^1P states of the Zn and Cd atom reagents,[33,34] although the ^3P states are sufficiently energetic to form OCdO and OZnO in exothermic reactions (Figure 10). Both OMO and MH_2 molecules[10,24,25] are made in these reactions, and we believe that OMO inserts into H_2 to form the HOMOH molecules, reaction 1. When a second H_2 molecule is present, the HMOH molecule can be formed.

$$M + O_2 + H_2 \rightarrow OMO + H_2 \rightarrow M(OH)_2 \ (M = Zn, Cd) \quad (1)$$

$$M + O_2 + 2H_2 \rightarrow MO + H_2O + H_2 \rightarrow HMOH + H_2O \quad (2)$$

Figure 10 shows the relative energies of the OZnO, OCdO reagent and $Zn(OH)_2$, $Cd(OH)_2$ product molecules, and the exothermic nature of the reactions (ΔE for reaction 1 is −111, −81, and −54 kcal/mol for M = Zn, Cd, and Hg, respectively, at the B3LYP level). Even though the Group 12 dioxide and dihydroxide molecules are stable, the Group 2 analogues are even more stable (for example $Ca(OH)_2$ is 181 kcal/mol more stable than $Ca + O_2 + H_2$).

The insertion reaction with H_2O_2 is straightforward, and the observation of the same product absorptions with the $O_2 + H_2$ and H_2O_2 reagents confirms our preparation of these $M(OH)_2$ molecules. The $Sr + H_2O_2$ reaction has been employed in the gas phase to form SrOH.[35] Here the energized $M(OH)_2$ molecule is relaxed by the matrix before decomposition to MOH can proceed.

$$M + HOOH \rightarrow HOMOH \quad (3)$$

Conclusions

Laser-ablated zinc and cadmium atoms were deposited with H_2 and O_2 in excess argon or neon and with O_2 in pure hydrogen or deuterium during deposition at 8 or 4 K. Full mercury arc irradiation excites metal atoms to insert into O_2 producing OMO molecules (M = Zn and Cd), which react further with H_2 molecules to give the metal hydroxides $M(OH)_2$ or HMOH and H_2O. The $M(OH)_2$ molecules were identified through O−H and M−O stretching modes with appropriate HD, D_2, $^{16,18}O_2$, and $^{18}O_2$ isotopic shifts. The HMOH molecules were characterized by O−H, M−H, and M−O stretching modes and an M−O−H bending mode, which were particularly strong in pure H_2 and D_2. Analogous Zn and Cd atom reactions with H_2O_2 in excess argon produced the same $M(OH)_2$ absorptions, which substantiates these assignments. DFT and MP2 calculations reproduce the IR spectra of these molecules. The bonding of Group 12 metal dihydroxides and comparison to Group 2 dihydroxides is considered. Although the Group 12 dihydroxide O−H stretching frequencies are lower, calculated charges show that the Group 2 dihydroxide molecules are more ionic.

Acknowledgment. We thank the National Science Foundation for support by Grant CHE 03-52487 and L. Khriachtchev for helpful suggestions on the use of urea-hydrogen peroxide.

References and Notes

(1) Cotton, F. A.; Wilkinson, G.; Murillo, C. A.; Bochmann, M. *Advanced Inorganic Chemistry*, 6th ed.; Wiley: New York, 1999.
(2) Holleman, A. F.; Wiberg, E. *Lehrbuch der Anorganischen Chemie*; Wiberg, N., Ed.; Walter de Gruyter: Berlin, 1995; Vol. 101, p 1389.
(3) Wang, X.; Andrews, L. *Inorg. Chem.* **2005**, *44*, 108 ($Hg(OH)_2$).
(4) Thompson, C. A.; Andrews, L. *J. Phys. Chem.* **1996**, *100*, 12214 ($Be(OH)_2$).
(5) (a) Andrews, L., Wang, X. *Inorg. Chem.* **2005**, *44*, 11. (b) Wang, X.; Andrews, L. *J. Phys. Chem. A* **2005**, *109*, 2782.
(6) Kauffman, J. W.; Hauge, R. H.; Margrave, J. L. *High Temp. Sci.* **1984**, *18*, 97.
(7) Macrae, V. A.; Greene, T. M.; Downs, A. J. *Chem. Phys. Phys. Chem.* **2004**, 4586.
(8) Andrews, L.; Citra, A. *Chem. Rev.* **2002**, *102*, 885.
(9) Andrews, L. *Chem. Soc. Rev.* **2004**, *33*, 123.
(10) Wang, X.; Andrews, L. *J. Phys. Chem. A* **2004**, *108*, 11006 (Zn, Cd + H_2).
(11) Pettersson, M.; Tuominen, S.; Rasanen, M. *J. Phys. Chem. A* **1997**, *101*, 1166.
(12) Pehkonen, S.; Pettersson, M.; Lundell, J.; Khriachtchev, L.; Rasanen, M. *J. Phys. Chem. A* **1998**, *102*, 7643.
(13) Frisch, M. J.; Trucks, G. W.; Schlegel, H. B.; Scuseria, G. E.; Robb, M. A.; Cheeseman, J. R.; Zakrzewski, V. G.; Montgomery, J. A., Jr.; Stratmann, R. E.; Burant, J. C.; Dapprich, S.; Millam, J. M.; Daniels, A. D.; Kudin, K. N.; Strain, M. C.; Farkas, O.; Tomasi, J.; Barone, V.; Cossi, M.; Cammi, R.; Mennucci, B.; Pomelli, C.; Adamo, C.; Clifford, S.; Ochterski, J.; Petersson, G. A.; Ayala, P. Y.; Cui, Q.; Morokuma, K.; Malick, D. K.; Rabuck, A. D.; Raghavachari, K.; Foresman, J. B.; Cioslowski, J.; Ortiz, J. V.; Stefanov, B. B.; Liu, G.; Liashenko, A.; Piskorz, P.; Komaromi, I.; Gomperts, R.; Martin, R. L.; Fox, D. J.; Keith, T.; Al-Laham, M. A.; Peng, C. Y.; Nanayakkara, A.; Gonzalez, C.; Challacombe, M.; Gill, P. M. W.; Johnson, B.; Chen, W.; Wong, M. W.; Andres, J. L.; Gonzalez, C.; Head-Gordon, M.; Replogle, E. S.; Pople, J. A. *Gaussian 98*, revision A.6; Gaussian, Inc.: Pittsburgh, PA, 1998.
(14) Milligan, D. E.; Jacox, M. E. *J. Mol. Spectrosc.* **1973**, *46*, 460.
(15) (a) Andrews, L.; Ault, B. S.; Grzybowwski, J. M.; Allen, R. O. *J. Chem Phys.* **1975**, *62*, 2461. (b) Wight, C. A.; Ault, B. S.; Andrews, L. *J. Chem. Phys.* **1976**, *65*, 1244.
(16) Jacox. M. E.; Milligan, D. E. *J. Mol. Spectrosc.* **1972**, *42*, 495.
(17) Smith, D. W.; Andrews, L. *J. Chem. Phys.* **1974**, *60*, 81.
(18) Jacox, M. E.; Thompson, W. E. *J. Chem. Phys.* **1994**, *100*, 750.
(19) Thompson, W. E.; Jacox, M. E. *J. Chem. Phys.* **1989**, *91*, 3826.
(20) Zhou, M. F.; Hacaloglu, J.; Andrews, L. *J. Chem Phys.* **1999**, *110*, 9450.
(21) Wang, X.; Andrews, L. *J. Phys. Chem. A* **2001**, *105*, 5812.
(22) Wang, X.; Andrews, L. *J. Phys. Chem. A* **2004**, *108*, 1103.
(23) (a) Andrews, L.; Wang, X. *J. Phys. Chem. A* **2004**, *108*, 3879. (b) Andrews, L.; Wang, X. *J. Chem. Phys.* **2004**, *121*, 4724.
(24) Chertihin, G. V.; Andrews, L. *J. Chem. Phys.* **1997**, *106*, 3457 (ZnO_2 and CdO_2).
(25) Greene, T. M.; Brown, W.; Andrews, L.; Downs, A. J.; Chertihin, G. V.; Runeberg. N.; Pyykko, P. *J. Phys. Chem.* **1995**, *99*, 7925 (ZnH_2 and CdH_2 in solid argon).
(26) Bauschlicher, C. W., Jr.; Langhoff, S. R.; Partridge, H. *J. Chem. Phys.* **1986**, *84*, 901.
(27) Koput, J.; Peterson, K. A. *J. Phys. Chem. A* **2002**, *106*, 9595 and references therein.
(28) (a) Pereira, R.; Levy, D. H. *J. Chem. Phys.* **1996**, *105*, 9733. (b) Levy, D. H., 2004, personal communication.
(29) Lagarde, P.; Nerenberg, M. A. H.; Farge, Y. *Phys. Rev. B* **1973**, *8*, 1731.
(30) Rosenbaum, N. H.; Owrutsky, J. C.; Tack, L. M.; Saykally, R. J. *J. Chem. Phys.* **1986**, *84*, 5308.
(31) Huber, K. P.; Herzberg, G. *Constants of Diatomic Molecules*; Van Nostrand: Princeton, 1979.
(32) Kaupp, M.; Schleyer, P. v. R. *J. Am. Chem. Soc.* **1992**, *114*, 491.
(33) Moore, C. E. *Atomic Energy Levels*, Circular 467; National Bureau of Standards: Washington, DC, 1952.
(34) Ault, B. S.; Andrews, L. *J. Mol. Spectrosc.* **1977**, *65*, 102.
(35) Presunka, P. I.; Coxon, J. A. *J. Chem. Phys.* **1994**, *101*, 201.